GeoPlanning
Journal of Geomatics and Planning
Geoplanning: Journal of Geomatics and Planning, Vol. 12, No. 2, 2025, 197 - 214

e-ISSN: 2355-6544

Received: 29 August 2024;
Revised: 14 May 2025;
Accepted: 25 October 2025;
Available Online: 31 October 2025;
Published: 31 October 2025.

Keywords:
Wildfire Susceptibility Index, Weighted Overlay Analysis, Image Analysis, Table Mountain National Park

*Corresponding author(s)
email: patroba.odera@uct.ac.za

Original Research Open access

Modelling Spatial-Temporal Wildfire Susceptibility Using Geospatial Techniques Over the Table Mountain Nature Reserve, South Africa

Syed Tanweer Raza Nujjoo[1], Patroba Achola Odera[1]*

1. *Division of Geomatics, School of Architecture, Planning and Geomatics, University of Cape Town, South Africa*

DOI: 10.14710/geoplanning.12.2.197-214

Abstract

Mountains in Cape Town are generally highly susceptible to wildfire due to the hot-dry summer months and various climatological factors that could aggravate the situation. In fact, the Cape Floral Kingdom in Table Mountain National Park is categorized as the world's hottest floral hotspot. This study has utilized geospatial techniques to model spatial-temporal wildfire susceptibility over the Table Mountain Nature Reserve (TMNR) from 1978 to 2022 at a nearly 10-year interval epoch. This is achieved by first mapping and categorizing influential factors such as land use/land cover, aspect, temperature, slope, normalized difference vegetation index, precipitation, elevation, and wind speed. The categorized layers are then weighted and numerically integrated to determine wildfire susceptibility (WS) levels based on wildfire susceptibility index (WSI) over the TMNR. Results show that low WS levels occurred only in 1978, 1991 and 2014 with area coverage at 0.1% 0.01%, and 0.6% of the total area of TMNR, respectively. All the epochs contained moderate WS (24.5%; 24.8%; 4.4%; 32.6%; 4.0%), high WS (67.2%; 70.3%; 73.4%; 63.2%; 77.0%) and very high WS (8.2%; 4.9%; 22.2%; 3.6%; 19.0%) for 1978, 1991, 2002, 2014, and 2022, respectively. In general, results indicate increasing wildfire susceptibility over the TMNR, with the northern and western parts being the highly susceptible areas.

1. Introduction

Wildfires occur globally daily and have both positive and negative impacts on the environment. The positive impacts of wildfires include enhancement of biodiversity due to formation of open habitats by creating new wildlife habitats, natural pest control thus preventing diseases which could affect humans and animals, and regulation of the ecosystem. However, these positive impacts of wildfire cannot outweigh the devastating impacts of wildfires such as ecological imbalances, loss of human and animal lives, destruction of habitats and infrastructure, and air pollution (Lasslop et al., 2020; McLauchlan et al., 2020; Nones et al., 2024; Pausas & Keeley, 2021; Urbanski et al., 2008). Every year, fire takes place over the Table Mountain National Park (TMNP) from a natural source, prescribed burning for ecological benefits, or arson. The wildfire outbreak that shook the University of Cape Town community and citizens in the locality occurred on the 18th of April 2021. Shoko & Gayu (2021) highlighted the need for dynamic mapping to reduce wildfire risk and support mitigation planning.

The Table Mountain Nature Reserve, South Africa is only a portion of the TMNP, covering an area of about 5225 ha. The mountains and peaks are very susceptible to wildfires during the hot-dry summer months and become more hazardous during unpredictable coastal winds in Cape Town (Imray, 2021). Fuel loads, hot-

dry and windy weather, and a source of ignition are the three main constituents for triggering vegetation fires, and unfortunately, TMNP contains all three elements (van Wilgen, 2015). The topography of Table Mountain Nature Reserve (TMNR) is dominated by a Sandstone plateau reaching an altitude of about 1088 m. About 88% of TMNR consists of Fynbos, Renosterveld (5%), and Afro temperate forest (5%), and the remaining 2% comprises water bodies, trails, and a negligible number of built-up areas. Forsyth & van Wilgen (2008) and Cowling et al. (1996) agree that both Fynbos and Renosterveld are fire prone. On the Other hand, the Afro temperate forest is fire-resistant and regenerates mostly between fire intervals (Cowling et al., 1996). As per the soil metadata available on the City of Cape Town open data portal, TMNR is classified as one with limited pedological development. The soil is characterized as the most shallow, acidic, mainly sandy, and nutrient poor on the sandstone plateau, whereas deeper and richer nutrients are found on the shale and granite slopes (Cowling et al., 1996).

The study area experiences wet-winter (June-August) and dry-summer (November-February). The resulting dry summer climate is due to the diversion of the southeasterly wind caused by the high-pressured ridging cells in the Atlantic Ocean, resulting to the loss of moisture in the wind captured from the Indian Ocean in that process (Cowling et al., 1996). Additionally, Forsyth & van Wilgen (2008) reported that 90.5% of the area burnt on TMNP occurred in summer (November-February) or autumn (March-May).

Previous wildfire-related research conducted over the TMNP includes assessments and trends of fire regimes (Chapungu et al., 2024; Forsyth & van Wilgen, 2008), and fire hazard risk analysis (Defratti et al., 2015). These studies have provided important data and information regarding fire occurrences and behaviors on the TMNP. However, none of the existing studies have modelled spatial-temporal wildfire susceptibility (WS) over the TMNP, the same applies to the TMNR which is part of the TMNP. Spatial-temporal wildfire susceptibility models would provide a better understanding of the spatial distribution of WS over the years and possible future trends.

This study carries out spatial-temporal WS modelling using multicriteria weighted overlay analysis over the TMNR by incorporating wildfire conditioning factors such as precipitation, temperature, elevation, slope, aspect, land use/land cover (LULC), normalized difference vegetation index (NDVI) and wind speed. The eight factors are mapped, weighted and scaled to enable spatial-temporal WS modelling using multicriteria weighted overlay analysis by incorporating wildfire conditioning criteria from previous related studies in other parts of world such as Herenna forest in Ethiopia (Suryabhagavan et al., 2016), Galicia in Spain (Novo et al., 2020), Ören in Turkey (Kavlak et al., 2021), Mediterranean regions (Sivrikaya & Küçük, 2022) and Raja Musa Forest in Malaysia (Ya'acob et al., 2022). Each of the eight factors is reclassified into five classes (very low, low, moderate, high and very high) depending on the influence range on WS

This study aims to identify the level of forest fire vulnerability in TMNR. With the help of GIS and remote sensing technology, spatial-temporal modeling of forest fire vulnerability over a period of 44 years (1978-2022) in a span of nearly 10 years was carried out by identifying and combining various factors that drive forest fires. Through the development of an integrated spatial-temporal model utilizing weighted overlay analysis and advanced geospatial techniques, the results are expected to provide a more accurate and timelier scientific basis for conservation authorities in formulating fire risk mitigation strategies.

2. Data and Methods

2.1. Study Area

The study area (see Figure 1) is an integrated part of Table Mountain National Park (TMNP), which focuses on Table Mountain Nature Reserve (TMNR). Geographically, the study site covers approximately 5,255 hectares, located within the administrative boundaries of Cape Town, South Africa. Geographically and geomorphologically, the study area is dominated by sandstone highlands with a peak elevation of approximately 1,088 meters above sea level. The edaphic characteristics of the area are characterized by shallow, sandy, nutrient-poor, and acidic soils, indicating limited pedological development.

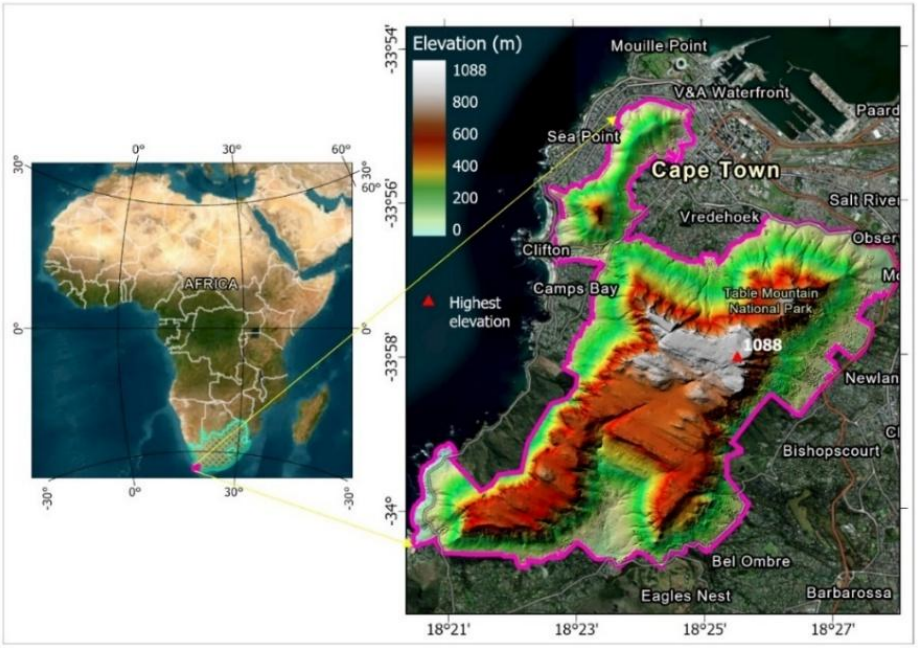

Source: Analysis, 2024; Google Maps 2024

Figure 1. Location Map of the Study Area with its Undulating Terrain Depicted by the Lowest Elevation as Pale Green and Highest Elevation as Pale Grey. The TMNR (Pink Outline) is Situated within the City of Cape Town and Peaks at 1088 m Above the Mean Sea Level

This region is under the influence of a Mediterranean climate characterized by intense dry and hot summers and wet winters. These conditions are the main factors causing forest fires, especially during the period from November to February. In addition, the dominance of vegetation such as the Fynbos biome/shrubbery (88%) and Renosterveld vegetation (5%) is one of the triggers for the fire cycle in the TMNR area (see Figure 2). This is because both vegetation types are pyrophilic (fire-prone) and, combined with the weather conditions in the study area, collectively produce a high fuel load.

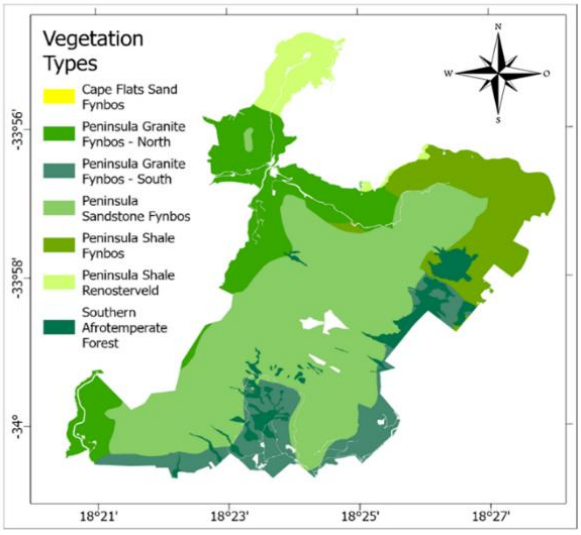

Source: Analysis, 2024

Figure 2. Spatial Distribution of Vegetation Types Over the TMNR: White Holes and Veins Represent Water Bodies, Roads, and trails

2.2. Datasets

The main phases and related datasets applied in this research are outlined in Figure 3. The identification and modelling of spatial-temporal variability of wildfire susceptibility (WS) followed three main phases: data acquisition, data preparation and processing, and data modelling and validation. Table 1 displays detailed attributes of the remotely sensed data over the TMNR. The intervals between each epoch for the final data acquired (1978, 1991, 2002, 2014, and 2022) were 10 ± 3 years, constrained by availability of reliable data.

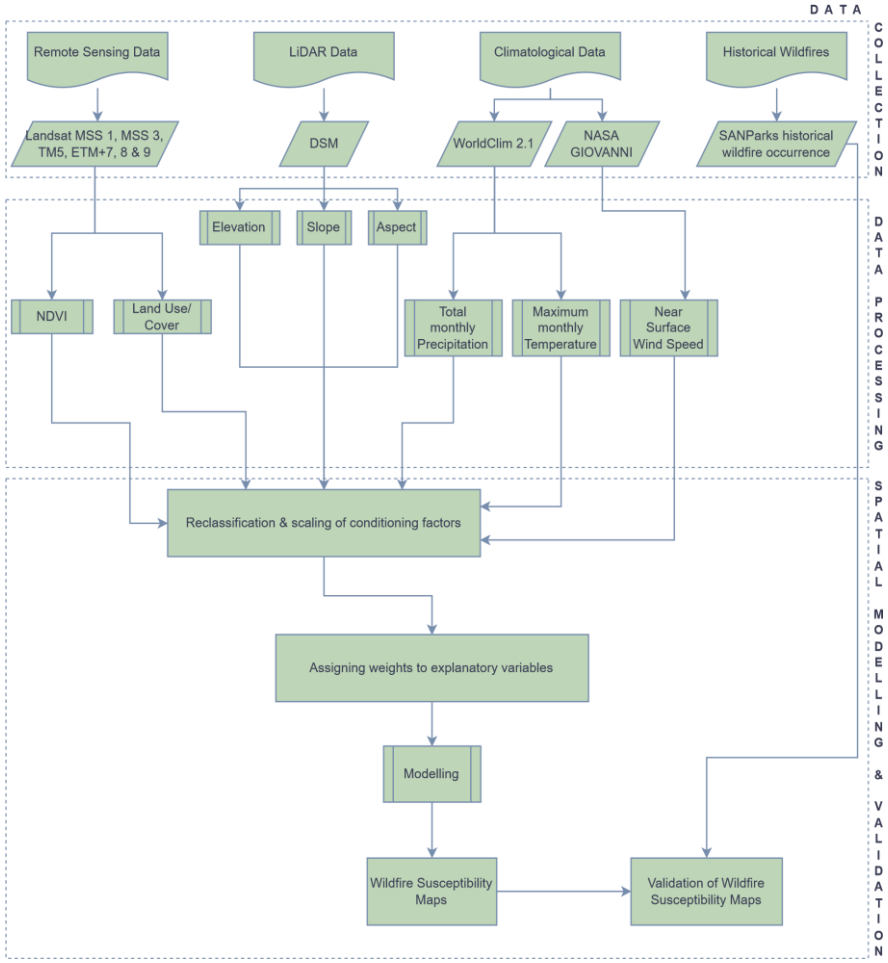

Source: Analysis, 2024

Figure 3. Flowchart Diagram

Table 1. Remotely Sensed Data Acquired from the United States Geological Survey (USGS) Earth Explorer repository (https://earthexplorer.usgs.gov/)

Acquired Imagery	Path/Row	Resolution (m)	Acquisition Period
Landsat 3 MSS	187/84	60	19/12/1978
Landsat 5 TM	175/84	30	25/03/1991
Landsat 7 ETM+	175/84	30	15/02/2002
Landsat 8 OLI/TIRS	175/84	30	25/04/2014
Landsat 9 OLI/TIRS	175/84	30	18/02/2022

**) Note: The resolution attribute refers to the spatial resolution/ pixel size of each satellite imagery.*

Source: Analysis, 2024

To analyze wildfire spread, LiDAR DSM considered superior to existing satellite DEMs over the study area (Malindi & Odera, 2021) was used. Climatological data used in this study are presented in Table 2. Historical fire datasets used for validation were obtained from the South African National Parks (SANParks). The fire data are provided as individual polygon shape files for each year, spanning from 1962 to 2021. Within TMNP, there has been a total of 747 historical fire events, with 276 occurrences specifically on the TMNR area, accounting for approximately 37% of the total fire outbreaks over the entire TMNP.

Table 2. Climatological Data Obtained from Online Services and Local Meteorological Stations

Variable	Data Source	Data Format	Spatial Resolution	Temporal Resolution
Online Services				
Precipitation (mm)	WorldClim 2.1 (https://www.worldclim.org/data/monthlywth.html)	GeoTiff raster grid data	2.5' (~21km^2)	Monthly Total
Maximum Temperature (°C)	WorldClim 2.1 (https://www.worldclim.org/data/monthlywth.html)	GeoTiff raster grid data	2.5' (~21km^2)	Monthly Average
Near Surface Wind Speed (m/s)	GIOVANNI-NASA (https://giovanni.gsfc.nasa.gov/ giovanni/)	GeoTiff raster grid data	0.25° (~773km^2)	Monthly Average
Meteorological Stations				
Daily Rainfall (mm)	South African Weather Service	CSV	n/a	Monthly Total
Daily Maximum Temperature (°C)	South African Weather Service	CSV	n/a	Monthly Average
Wind Speed (m/s)	South African Weather Service	CSV	n/a	Monthly Average

**) Note: All the variables were consistently acquired with a monthly temporal resolution. Note that the intention to acquire climatological data from the online services was solely to procure precipitation, temperature, and wind speed data.*

Source: Analysis, 2024

2.3. Data Processing

An object-based support vector machine (SVM) classification was used to classify each aerial imagery specified in Table 1 into five classes (water bodies, built-up areas, forest and thicket, shrub land, and grass land). An accuracy assessment was then performed using reference data extracted from high resolution satellite imagery (https://cityimg.capetown.gov.za/erdas-iws/esri/GeoSpatial%20Datasets/rest/services/) for each LULC class for the respective epochs. The Overall Accuracy and Kappa hat Coefficient for 1978 classified image was 88% and 0.9, respectively, 1991 (86% and 0.8), 2002 (80% and 0.7), 2014 (85% and 0.8), and 2022 (76% and 0.7). The ranges of Overall Accuracies (76 – 88%) and Kappa hat Coefficients (0.7 – 0.9) indicate no vast deviations in the accuracies, and the high accuracy values indicate that these images are applicable for the current analysis.

NDVI is one of many indices which focuses on the numerical indication of the greenness of vegetation based on the red (R) and near-infrared (NIR) bands of the electromagnetic spectrum (Velizarova et al., 2017). The mathematical equation for calculating NDVI index is expressed in Equation 1 (Carlson & Ripley, 1997). The resulting NDVI maps were reclassified with the lower indices indicating drier vegetation hence higher WS, and larger indices indicating healthier vegetation hence lower WS.

$$NDVI = \frac{NIR-R}{NIR+R} \quad \text{..... (Equation 1)}$$

The rate of spread of fire is influenced by slope, and fire moves more rapidly uphill than downhill (Defratti et al., 2015). Consequently, steeper slopes are reclassified as having higher WS zones than gentle slopes. Another factor is aspect, defined as the direction to which the slope is facing and is typically categorized as flat and other cardinal-ordinal directions. In the southern hemisphere, generally northern-facing slopes are mostly exposed to the sun, hence are high in temperature, and consist of drier vegetation (Defratti et al., 2015).

Precipitation is an important factor, as pre-fire or in-fire season rainfall would impact on the extent and severity of the wildfire (Holden et al., 2018). Logically, low precipitation would indicate dry vegetation, thus making it highly susceptible to fire, while the opposite is true. High temperatures quicken the ignition and burning processes as less thermal energy is required to set the fuel ablaze (Pausas & Keeley, 2021). Cruz & Alexander (2019) observed that the effect of the spread of wildfire based on wind speed is quite complex as it is also dependent on factors such as the characteristics of the fuel, vertical wind speed and intensity, and the initial intensity of the ignition itself.

2.3. Weighted Overlay Analysis

Weighted overlay analysis is a technique that integrates reclassified rasters onto a standardized scale, assigning rank values to class values for each raster along with their corresponding percentage influence (Mayfield et al., 2015). This approach is widely employed, as evidenced by most related articles reviewed, namely, Sivrikaya & Küçük (2022), Ya'acob et al. (2022), Abdo et al. (2022), Kavlak et al. (2021), Kumari & Pandey (2020), Suryabhagavan et al. (2016), and Pourtaghi et al. (2015). We applied wildfire susceptibility index (WSI) (see Equation 2) calculated by combining all the influential factors using a weighted linear combination equation as follows (Kayet et al., 2020; Tiwari et al., 2021),

$$WSI = \sum_{t=1}^{m} \sum_{f=1}^{n} (N W_t \times C_f) \quad \text{..... (Equation 2)}$$

where, NW_t is the normalized weight or % influence, C_f is the scale value, m is the number of variables, and n is the number of classes.

Table 3. Adopted and Derived Variables' Classes, Scale Value and % Influence Weight from Previous Studies Used for Reclassification and Modelling Purposes

Variable Raster	Influence (%)	Classes	Scale Value	Authors
Elevation (m)	6	>800; 600-800; 400-600; 200-400; <200	1; 2; 3; 4; 5 respectively	Adopted from Novo et al. (2020); Kumari & Pandey (2020); and Abdo et al. (2022)
Slope (°)	16	<5; 5-15; 15-25; 25-35; >35	1; 2; 3; 4; 5 respectively	Adopted from Novo et al. (2020)
Aspect	19	South (157.5°-157.5°); Southeast (112.5°-157.5°) and Southwest (202.5°-247.5°); East (67.5°-112.5°) and West (247.5°-292.5°); Flat (-1) and Northeast (22.5°- 67.5°); North (0°-22.5°, 337.5°-360°) and Northwest (292.5°-337.5°)	1; 2; 3; 4; 5 respectively	Derived from Tsiwari et al. (2021)
LULC	24	Water bodies; Built-up Areas; Forest and Thicket; Grass land; Shrub land	1; 2; 3; 4; 5 respectively	Partly adopted from Nuthammachot & Stratoulias (2021) and Suryabhagavan et al. (2016)
NDVI	10	>0.67; 0.54-0.67; 0.40-0.54; 0.27-0.40; <0.27	1; 2; 3; 4; 5 respectively	Adopted from Novo et al. (2020)
Total Monthly Precipitation(mm)	6	>31.3; 28.8-31.3; 26.3-28.8; 23.8-26.3; <23.8	1; 2; 3; 4; 5 respectively	Derived from Abdo et al. (2022)
Average Max. Temperature (°C)	16	<21.79; 21.79-22.58; 22.58-22.99; 22.99-23.40; >23.40	1; 2; 3; 4; 5 respectively	Adopted from Ya'acob et al. (2022)
Near Surface Wind Speed (m/s)	3	<3.65; 3.65-3.95; 3.90-4.30; 4.30-4.66; >4.66	1; 2; 3; 4; 5 respectively	Adopted from Abdo et al. (2022)

**) Note: The scale value represents very low WS (1), low WS (2), moderate WS (3), high WS (4), and very high WS (5). The % influence was solely derived based on a study by* Sivrikaya & Küçük (2022)*. The weights normalization employed this formula:* $\boldsymbol{NW_t = \frac{W_t}{\sum_{t=1}^{n} W_t} \times 100}$*, where* $\boldsymbol{NW_t}$ *is normalised weight or % influence;* $\boldsymbol{W_t}$ *is individual weight;* $t = 1, 2, ..., 8$.

Source: Analysis, 2024

The determination of wildfire susceptibility zones is influenced by factors of varying degrees of importance plus the scale value assigned to the discretized classes. Hence, different weights or percentage influence and scale value were adopted or derived from various authors who conducted the analytical hierarchy process (AHP) as proposed by Saaty (2004). Few derivations were necessary, mainly because of some research conducted in the northern hemisphere or simply because the study area did not possess comparable characteristics as TMNR. Table 3 presents the adopted or partially adopted and derived percentage influence, classes, and scale values for each criterion.

A visual validation for the WS maps or models was performed using historical in-situ fire data. The historical fire data acquired was merged into one shape file by using the 'Merge' tool, and then the centroid location for each polygon was extracted using the 'Feature to Point' tool, 0.5×0.5 km grids were processed over the study area using the 'Create Fishnet' tool, and the number of fire points located within a grid was manually updated into the attribute table. Ultimately, a dot layer representing the quantity of fire occurrences was created by altering the symbology of the centroid location of the grids using graduated symbols based on the number of fire occurrences per grid. This layer was then superimposed on the WS maps to allow for visual interpretations.

3. Results and Discussion

3.1. Reclassified Wildfire Susceptibility Factors Over the TMNR

Figure 4 shows the area covered by wildfire susceptibility zones based on LULC for the years 1978, 1991, 2002, 2014 and 2022. The spatial representation of wildfire susceptibility zones based on LULC is given in Figure 5. The TMNR landscape exhibits varied land cover classes, with water bodies and built-up areas being the least dominant (<2% of the total land area over the TMNR) since 1978. In terms of built-up areas, the trend appears constant because TMNR has very little infrastructure. Shrub land is the most dominant class throughout the years, with an average area of about 3236 ha (62%). The trend shows a noticeable drop in the area covered by forest and thicket from 1978 (24.5%) to 2022 (13.8%). This is largely attributed to the increase in grass land from 454 ha (8.7%) to 1029 ha (19.7%) over the study period. The grass land class also comprises of very dry grass, low dry sparse shrub land, bare land, rocky and sandy areas. An increase in trend for this category indicates a decrease in the other vegetation classes because of fire or any kind of de-vegetation.

Ordinarily, one would expect that the fire-driven fynbos biome would diminish. On the contrary, there are some types of fynbos which are very resilient to post-fire mortality and some which have rapid resprouting ability of about 4 months (Marais et al., 2014). Even the South African grass land biome has resprouting ability (Kruger et al., 1997), which means that the affected class would be forest and thicket. Another reason for the increase in the extent of grass land is attributed to the historical wildfire events over the TMNR and especially the burnt northeastern area due to the wildfire event in April 2021.

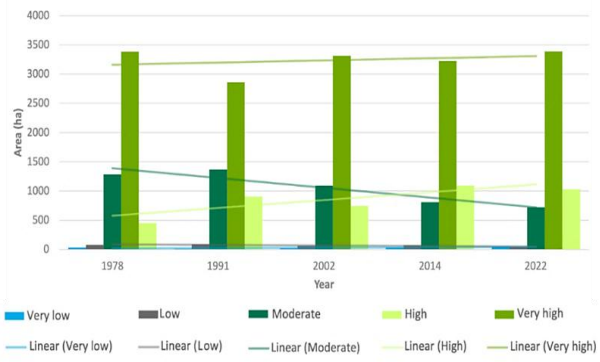

Source: Analysis, 2024

Figure 4. Area Coverage for WS Zones based on the Reclassified LULC Over the TMNR. WS Levels: Very Low (Water Bodies), Low (Built-Up Areas), Moderate (Forest and Thicket), High (Grass Land) and Very High (Shrub Land)

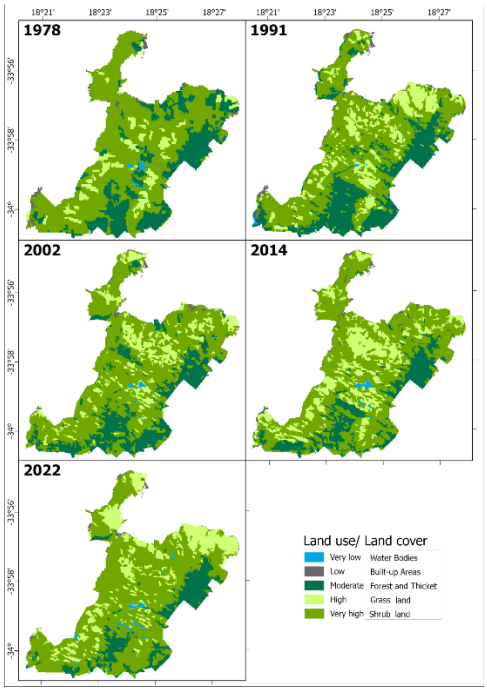

Source: Analysis, 2024

Figure 5. Spatial-Temporal Distribution of WS Zones based on the Reclassified LULC Over the TMNR. WS Levels: Very Low (Water Bodies), Low (Built-Up Areas), Moderate (Forest and Thicket), High (Grass Land) and Very High (Shrub Land)

The burnt scar is well noticed on the northeastern side of TMNR in the 2022 LULC map (depicted as grass land), which is also a high WS zone. The area covered by each WS level for LULC primarily depends on the versatility, growth rate, and type of vegetation cover. Built-up areas and water bodies, representing low and very low WS levels, respectively, are mostly static features with minimal changes over time. Therefore, the very high and high WS zones representing shrub land and grass land are found in an unpredictable manner across the study area. The moderate WS level representing forest and thicket is predominantly located in the southern and eastern parts of TMNR. The slow growth rate of forested areas helps maintain the moderate WS level in the same position, provided that no natural or man-made deforestation has occurred.

Reclassified NDVI maps based on classification scheme in Table 3 are shown in Figure 6. NDVI maps for 1991 and 2002 show presence of all the 5 WS levels with percentage area coverage for very low at 0.,9% and 0.003%, for 1991 and 2002 respectively, low (8.7% and 3.1%), moderate (14.7% and 12.8%), high (24.9% and 20.2%), and very high WS (50.7% and 63.9%). Very high WS zone is the most prevalent since 1978. In 1991, the very low, low, and moderate WS zones were mostly observed on the southern and eastern sides of the study area, where the Afro temperate forest is the dominant species. Similar comments made for the 1991 NDVI reclassified map apply to the 2002 NDVI reclassified map, with the exception that the low and very low WS zone are less extensive than the 1991 one.

Only four WS levels were observed in the 2022 reclassified NDVI map, and those were low (0.03%), moderate (9.5%), high (24.3%) and very high WS (66.2%). In 2022, the spatial pattern for the WS zones excluding the very high WS zone is highly correlated with the 2002 NDVI reclassified map, except that no very low WS zones were detected. So, this time, the Afro temperate forest was mostly zoned as moderate WS zone. In 1978 and 2014, only the moderate WS zone (0.1% and 1.2%, respectively), high (2.5% and 18.7%), and very high (97.4%; and 80.1%) were detected. In 1978, the moderate WS zone was only a small portion in the southern part of the TMNR within the high WS zone, located as minority patches in the southern and eastern parts of the study area (Figure 6). In terms of the spatial coverage for the WS zones, the 2014 NDVI reclassified map is similar to the 2002 NDVI reclassified map, excluding the very low and low WS levels.

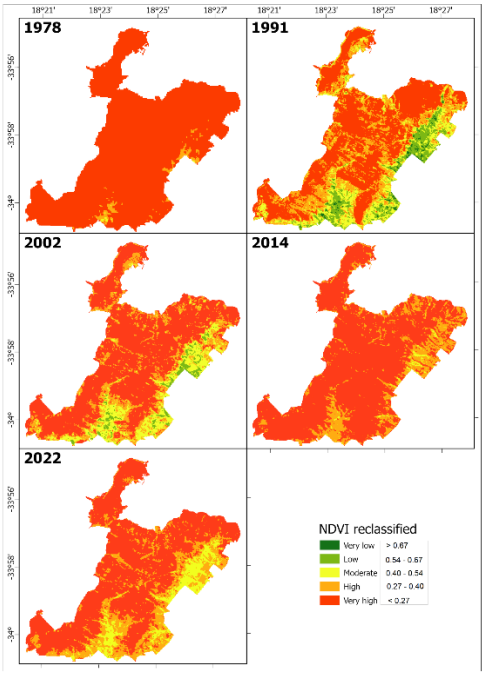

Source: Analysis, 2024

Figure 6. Spatial-Temporal Distribution of WS Zones based on the Reclassified NDVI Over the TMNR. WS Levels: Very Low (>0.67), Low (0.54-0.67), Moderate (0.40-0.54), High (0.27-0.40) and Very High (<0.27)

The area coverage for WS zones based on the NDVI reclassified maps from 1978 to 2022 is shown in Figure 7. The most dominant zone throughout each epoch was the very high WS zone, and fortunately, it is on a decreasing trend. However, despite the high and moderate WS zones being significantly less than the very high one in terms of the area extent covered on TMNR, they are both on an escalating trend. The very low and low WS zones, being the least dominant ones, are on a decreasing trend. So, the vegetation in the study area has been tending towards high-water stress mode over the years.

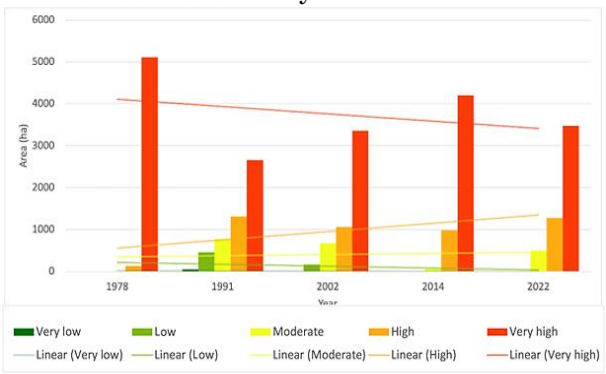

Source: Analysis, 2024

Figure 7. Area Coverage for WS Zones based on the Reclassified NDVI Over the TMNR. WS Levels: Very Low (>0.67), Low (0.54-0.67), Moderate (0.40-0.54), High (0.27-0.40) and Very High (<0.27)

Figure 8 illustrates the reclassified elevation map based on the parameters adopted from Table 3. The number of WS levels detected was 5 (very low, low, moderate, high, and very high WS zones). The most prevalent WS class was high with area coverage of 33.6%, followed by low (22.5%) and very high (17.5%) as shown in Figure 9. The least dominant WS levels were the very low (9.7%) followed by the moderate (16.7%). The spatial variations follow a concentric pattern due to the characteristics of mountainous areas whereby lower elevation areas are in the outer perimeter and elevation increases as it gets closer to the center. It is worth noting

that elevation does not vary over the years hence no temporal variations of WS levels in Figures 8 and 9. Wildfire susceptibility level increases with decrease in elevation over the TMNR.

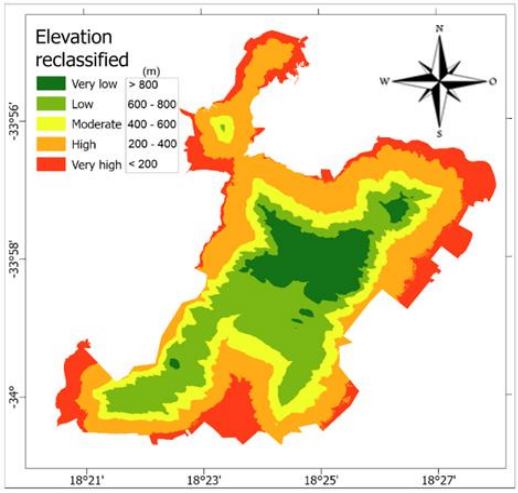

Source: Analysis, 2024

Figure 8. Spatial Distribution of WS Zones based on the Reclassified Elevation Over the TMNR. WS Levels: Very Low (>800), Low (600-800), Moderate (400-600), High (200-400) and Very High (<200 m)

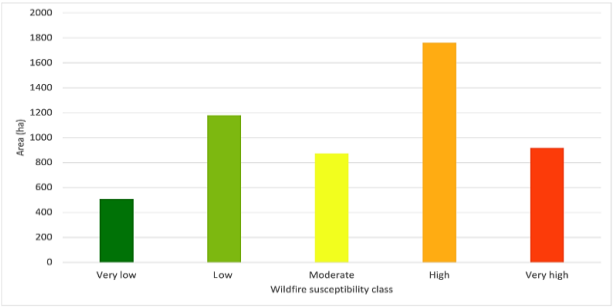

Source: Analysis, 2024

Figure 9. Area Coverage for WS Zones based on the Reclassified Elevation Over the TMNR. WS Levels: Very Low (>800), Low (600-800), Moderate (400-600), High (200-400) and Very High (<200 m)

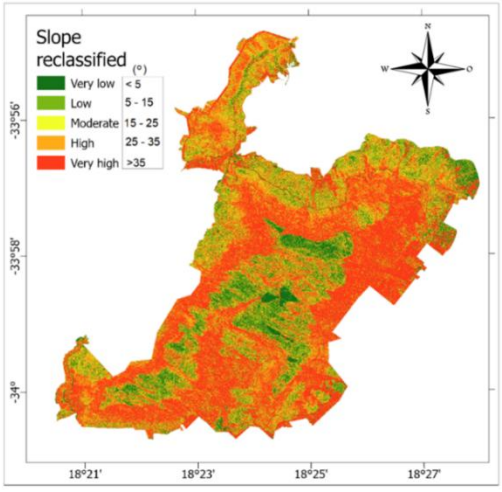

Source: Analysis, 2024

Figure 10. Spatial Distribution of WS Zones based on the Reclassified Slope Over the TMNR. WS Levels: Very Low (<5), Low (5-15), Moderate (15-25), High (25-35) and Very High (>35°)

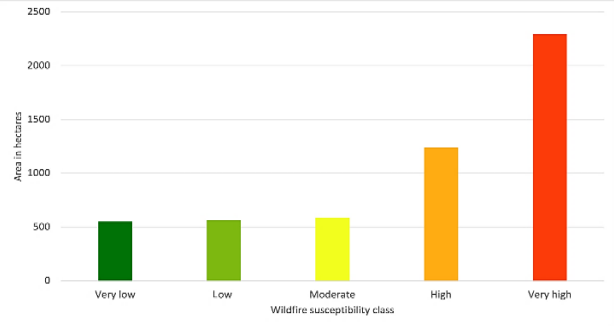

Source: Analysis, 2024

Figure 11. Area Coverage for WS Zones based on the Reclassified Slope Over the TMNR. WS Levels: Very Low (<5), Low (5-15), Moderate (15-25), High (25-35) and Very High (>35°)

Figure 10 illustrates the reclassified slope map based on the parameters adopted from Table 3 while Figure 11 shows the area covered by each WS zone. The very low WS zone covers 10.5% of the TMNR, low (10.8%) and moderate (11.2%). The high and very high WS zones (23.7% and 43.8%, respectively) cover a larger area than the other WS zones combined. The dominance of the resulting zones shows that, in general, TMNR is dominated by steep to very steep slopes. This spatial distribution pattern emphasizes that slope gradient is a factor that significantly influences the rate of fire spread in nature reserves. Thus, if slope gradient is the main factor, then almost the entire TMNR area falls into the category of high to very high vulnerability to forest fires.

Figure 12 displays the reclassified aspect map based on the parameters adopted from Table 3 while Figure 13 shows the extent covered by each WS zone depicted in Figure 12. The very low WS level coverage is 11.0%, low (22.2%), moderate (20.3%) and high (22.6%). The most dominant zone is the very high WS zone, which accounts for 24% of the total, mainly concentrated in the northern and western regions. This indicates that slope orientation significantly affects the level of vulnerability to forest fires because different levels of solar radiation also affect the level of dryness in TMNR. The spatial concentration of high and very high WS zones highlights areas that require prioritization of forest fire management planning.

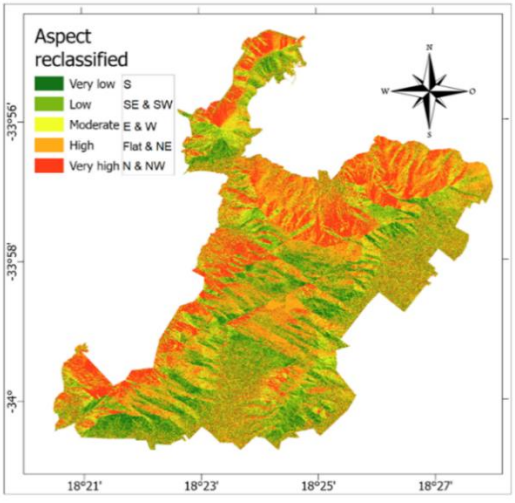

Source: Analysis, 2024

Figure 12. Spatial Distribution of WS Zones based on the Reclassified Aspect Over the TMNR. WS Levels: Very Low (South), Low (Southeast and Southwest), Moderate (East and West), High (Flat and Northeast) and Very High (North and Northwest)

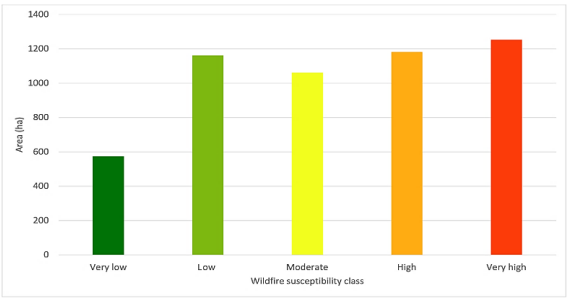

Source: Analysis, 2024

Figure 13. Area Coverage for WS zones based on the Reclassified Aspect Over the TMNR. WS Levels: Very Low (South), Low (Southeast and Southwest), Moderate (East and West), High (Flat and Northeast) and Very High (North and Northwest)

Figure 14 displays the reclassified total precipitation maps based on the parameters adopted from Table 3. The 1978 reclassified total precipitation map was the only map that consisted of four WS zones: very low (16.9%), low (16.9%), moderate (52.1%), and high (28.1%). For 1978, the very low and low WS classes are submerged within the moderate WS zone in the middle of the study area, extending from west to east. The high WS level is located on the far northeastern, southeastern, southwestern, and northwestern sides of TMNR. The very high WS zone was the only WS level detectable in the 1991 and 2002 reclassified total precipitation maps. In 2014 and 2022, only the high WS zone (40.4% and 96.6%) and moderate WS zone (59.6% and 3.4%), respectively, were detectable. In 2014, the northern, southwestern, and a small portion of the southeastern TMNR were represented by the high WS zone, while the remaining area was covered by the moderate WS zone. In 2022, the map was predominantly covered by the high WS zone, with dot-patterns from west to east representing the moderate WS zone.

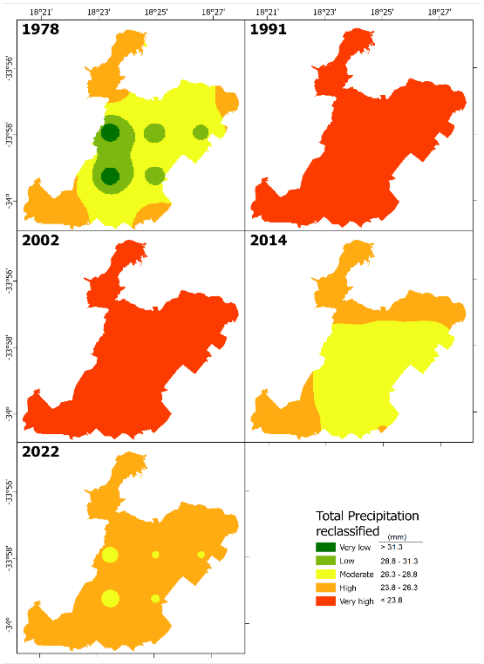

Source: Analysis, 2024

Figure 14. Spatial-Temporal Distribution of WS Zones based on the Reclassified Total Precipitation Over the TMNR. WS Levels: Very Low (>31.3), Low (28.8-31.3), Moderate (26.3-28.8), High (23.8-26.3) and Very High (<23.8 mm)

A graphical representation of the area distribution of total precipitation is depicted in Figure 15. Even though the very high WS zone was the dominant zone in 1991 and 2002, it is apparently on a declining trend.

However, this observation is inconclusive as a two-data-point trend is statistically unreliable. Similarly, the moderate WS zone shows a decreasing trend, albeit the rise in total precipitation for that zone in the year 2014. The very low and low WS zones are unquestionably in a depressing mode. So, the only escalating zone is the high WS zone, despite being unidentified for the years 1991 and 2002.

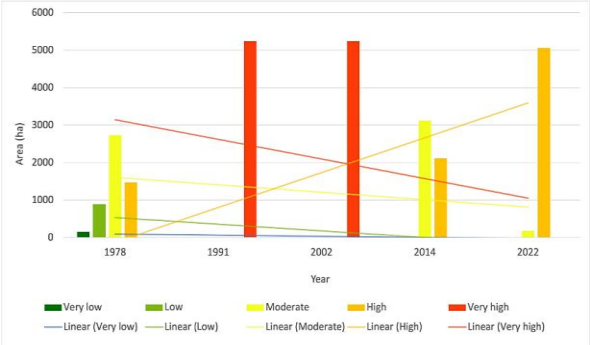

Source: Analysis, 2024

Figure 15. Area Coverage for WS zones based on the Reclassified Total Precipitation Over the TMNR. WS Levels: Very Low (>31.3), Low (28.8-31.3), Moderate (26.3-28.8), High (23.8-26.3) and Very High (<23.8 mm)

Figures 16 and 17 display the reclassified average monthly maximum temperature map and graph, respectively, based on the parameters adopted from Table 3. Five WS classes were detected in the 1978 and 2014 reclassified mean maximum temperature maps, including very low WS zone covering 5.1% and 8.3%, low WS (27.3% and 51.3%), moderate (16.2% and 24.3%), high (25.3% and 12.1%), and very high (26.0% and 4.0%). The 1991 reclassified mean maximum temperature map is composed of four WS zones, namely low (0.4%), moderate (2.6%), high (5.7%), and very high (91.3%), which covered almost the entire TMNR. The 2002 reclassified mean maximum temperature map had three WS zones, with moderate (0.2%), high (2.5%), and very high (97.3%), while the 2022 reclassified mean maximum temperature map is comprised of only the very high WS zone.

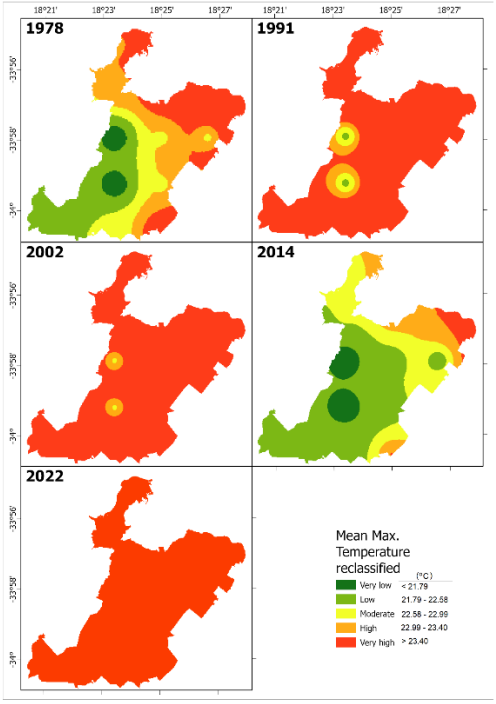

Source: Analysis, 2024

Figure 16. Spatial-Temporal Distribution of WS Zones based on the Reclassified Mean Maximum Temperature Over the TMNR. WS Levels: Very Low (<21.79), Low (21.79-22.58), Moderate (22.58-22.99), High (22.99-23.40) and Very High (>23.40 °C)

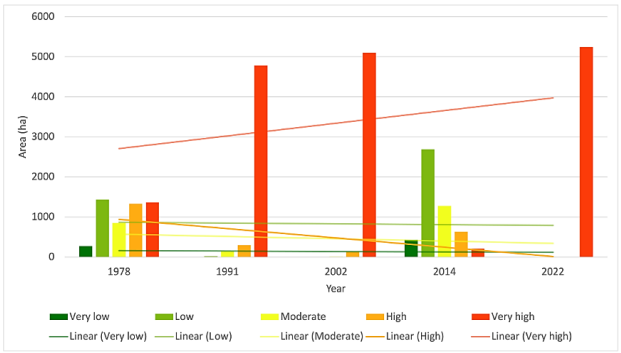

Source: Analysis, 2024

Figure 17. Area Coverage for WS Zones based on the Reclassified Mean Maximum Temperature Over the TMNR. WS Levels: Very Low (<21.79), Low (21.79-22.58), Moderate (22.58-22.99), High (22.99-23.40) and Very High (>23.40 °C)

In addition, the very high WS zone for mean maximum temperature is escalating quite rapidly, while the rest of the other lower WS levels are gradually decreasing over the study period (Figure 17). Finally, there were no spatial variations detected for the reclassified near surface wind speed, the entire area of study was classified as very high WS zone for all epochs, due to the nearly uniform high wind speed in the study area. Hence, no figural depictions were necessary.

3.2. Composite Spatial-Temporal Wildfire Susceptibility Models and Validation Over the TMNR

The output of the weighted overlay analysis is shown in Figure 18 and graphically presented in Figure 19. In Figure 18, The centroid location for each dot explains the number of fire events to an extent of 0.5 × 0.5 km. Some circles appear outside the study area due to their centroid locations being near the edge. The dots appear in multiple spots over TMNR, except for the dot representing 5, 11, and 13, which appeared only once.

There is no very low WS over the study area since 1978. The low WS zone with WSI range: 2.26-2.62 occurred in the epoch years 1978 (8 ha| 0.1%), 1991 (0.27 ha| 0.01%), and 2014 (30 ha| 0.6%). All the epochs contained moderate WS zone with WSI range: 2.63-3.54 (1,254 ha| 24.5%; 1,289 ha| 24.8%; 226 ha| 4.4%; 1,686 ha| 32.6%; 206 ha| 4.0%), high WS zone with WSI range: 3.54-4.53 (3,439 ha| 67.2%; 3,650 ha| 70.3%; 3,815 ha| 73.4%; 3,269 ha| 63.2%; 3,982 ha| 77.0%) and very high WS zone with WSI range: 4.540-4.964 (419 ha| 8.2%; 253 ha| 4.9%; 1,157 ha| 22.2%; 185 ha| 3.6%; 982 ha| 19.0%) for 1978, 1991, 2002, 2014, and 2022, respectively. The maps for 2002 and 2022 have the moderate WS zone as their lowest (Figure 19).

In the 1978 WS map, the low WS zone is centrally located where the water bodies are situated. The moderate WS zone is predominantly located on the higher elevations over the TMNR, where the low dry sparse shrub land could be found. There were also a few areas representing the moderate WS zone on the lower elevations and on the southern part of the study area. The high WS areas surrounded TMNR mainly on its lower elevation areas while the very high WS zone is in the northern region. In the 1991 WS map, the low WS zone might not be visible at the plotting scale due to the very small area it covered, but it is confirmed to be located where a water body is situated. The moderate WS zone is spatially intersected with the forested areas, wetlands, and water bodies. This WS zone is distributed predominantly on the southern and eastern parts of the TMNR. Furthermore, the high WS zone covered almost the entire TMNR, but was more dominant on the northern and western sides of the study area. In the 2002 WS map, the moderate WS areas were once again represented by the water bodies and a minimal portion of the southeastern part of the study area. The high WS zone was the dominant one, covering almost the entire study area, and the very high WS zone was predominantly detected in the northern and western parts of TMNR. In the 2014 WS map, the low WS zone was mainly detected on/near water bodies.

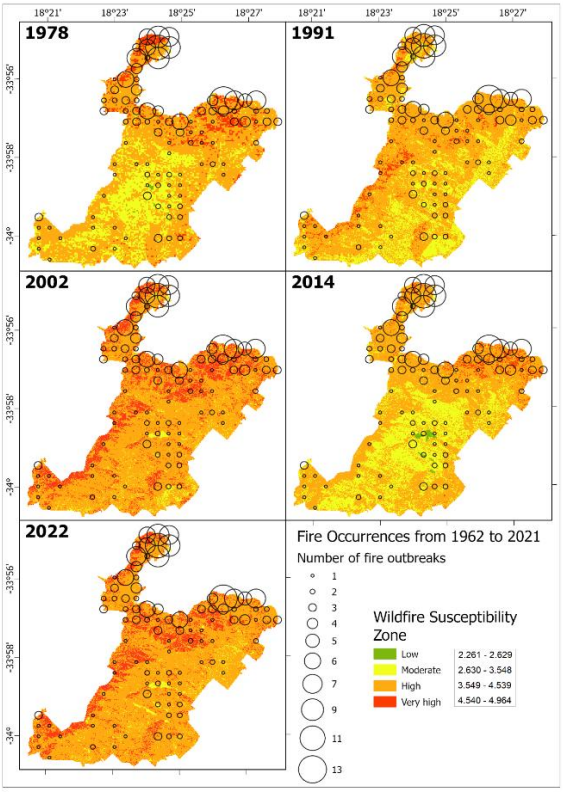

Source: Analysis, 2024

Figure 18. Spatial-Temporal Distribution of Wildfire Susceptibility Zones Over the TMNR based on the Modelled Wildfire Susceptibility Index. Circles Overlaid Represent the Fire Occurrences from 1962 to 2021, with the Size Indicating the Number of these Fire Events. WS Levels based on WSI: Low (2.26-2.62), Moderate (2.63-3.54), High (3.54-4.53) and Very High (4.54-4.96)

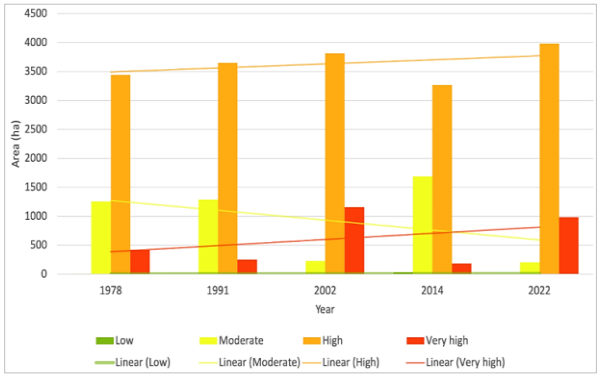

Source: Analysis, 2024

Figure 19. Area Coverage for WS Zones Over the TMNR based on the Modelled Wildfire susceptibility index. WS levels based on WSI: Low (2.26-2.62), Moderate (2.63-3.54), High (3.54-4.53) and Very High (4.54-4.96)

The moderate and high WS zone for 2014 is similar to 1978, indicating high spatial correlation in WS level for 1978 and 2014, with the exception that the 2014 WS map was slightly less intense in terms of the WS levels. Additionally, the very high WS zone was found on the northeast side of the study area. In general, high, and very high WS levels are escalating quite rapidly over the entire study period. Consequently, the TMNR is becoming more and more prone to wildfire occurrences (Figure 19). In addition, the regions that must be highly monitored are in the northern and western parts of the TMNR.

The black circles in Figure 18 are the validation locations of historical fire occurrences from 1962 to 2021. The historical fire events indeed attested to a high frequency of fire occurrences in the northern and western parts of the TMNR, where the zones have been classified as high and very high WS zones for all the epochs. From this analysis, it can be confirmed that areas around Signal Hill and Lion's Head are the most wildfire susceptible and vulnerable regions over the TMNR. Although wildfire vulnerability is not the subject of this study, it is possible to infer high wildfire vulnerability over areas around Signal Hill and Lion's Head as they are frequently visited by people due to their scenic views at the peaks. The increasing trend of built-up areas can be seen as a potential correlator for more people to access identified wildfire hotspots. Moreover, the areas where few wildfire events have been observed despite being in the high and very high WS zones, could still be future potential threat. In general, this visual validation is considered satisfactory despite limited ground data in terms of spatial and temporal coverage.5

The results of forest fire vulnerability modelling prove that a combination of factors such as climate, vegetation type and topographical conditions influence the level of forest fire vulnerability. This is in line with previous studies conducted in various regions, such as the Mediterranean region (Sivrikaya & Küçük, 2022), the Herenna Forest in Ethiopia (Suryabhagavan et al., 2016), the Raja Musa Forest in Malaysia (Ya'acob et al., 2022), Ören in Turkey (Kavlak et al., 2021), and Galicia in Spain (Novo et al., 2020). These studies have successfully identified the factors that influence the occurrence of forest fires. These consistent findings indicate that the factors triggering fires used in the study are relevant and in line with empirical findings in previous studies.

The findings of this study further confirm that spatial and temporal variations through a weighted overlay analysis approach are effective in determining the level of fire hazard vulnerability. This approach supports the findings of previous studies that emphasize the importance of integrating determining factors into a single spatial analysis framework to produce comprehensive fire hazard vulnerability maps. Thus, the results of this study not only reinforce the findings of previous studies, but also expand their application in the context of area conservation as a basis for forest fire management and mitigation, such as in Table Mountain Nature Reserve.

4. Conclusion

This analysis sought to identify the degree of wildfire susceptibility over the TMNR. With the aid of GIS and remote sensing technologies, a spatial-temporal modelling of the wildfire susceptibility over a period of 44 years (1978-2022) in a near 10-year epoch was conducted by identifying and incorporating various wildfire driving factors. To achieve this task, the common and main influential factors such as LULC, aspect, mean maximum temperature, slope, NDVI, total precipitation, elevation, and near surface wind speed have been applied at scales and weights in a multilayer weighted analysis to obtain the spatial-temporal wildfire susceptibility levels. The final integrated model is categorized into four wildfire susceptibility levels (low, moderate, high and very high) as no very low wildfire susceptibility (WS) zone was obtained from the weighted overlay analysis for the entire period of the study.

The lowest susceptibility level is the low WS zone observed in 1978 covering an area of 8 ha, 1991 (0.27 ha), and 2014 (30 ha) but none in 2002 and 2022. All the epochs contain moderate WS zone at 1,254 ha in 1978, 1,289 ha (1991), 226 ha (2002), 1,686 ha (2014) and 206 ha (2022); high WS zones at 3,439 ha in 1978, 3,650 ha (1991), 3,815 ha (2002), 3,269 ha (2014) and 3,982 ha (2022); and very high WS zone at 419 ha in 1978, 253 ha (1991), 1,157 ha(2002), 185 ha (2014) and 982 ha (2022). These results show an escalating trend in the high and very high WS zones and a depressing trend in the moderate WS zones. The low WS zone was unfortunately negligible on TMNR, implying that the study area is becoming progressively more susceptible to wildfire occurrences (especially in the northern and western parts of the TMNR as confirmed through validation).

This research has demonstrated the power of spatial modelling in mapping semi-dynamic wildfire susceptibility over the TMNR. Results provide the first continuous surface distribution of WS zones over the TMNR at different levels, rather than ground observation datasets that are only available at discrete points, with low spatial and temporal resolutions. Spatial-temporal wildfire susceptibility variations obtained in this research

provide a better understanding of the spatial distribution of WS over the years and possible future trends to facilitate informed decision-making regarding wildfire preventive and mitigation planning. The findings of this research will support optimal wildfire surveillance and mitigation initiatives over the TMNR. Based on the results, it is highly recommended that wildfire surveillance systems be installed in the northern and western parts of the TMNR and most definitely in strategic locations over Signal Hill and Lion's Head, as these areas are situated in the very high and high WS zones. Our next study will be based on predictive wildfire modelling to facilitate wildfire mitigation planning for potential future wildfire occurrences over the TMNR.

5. Acknowledgments

The following organizations are appreciated for making relevant data freely available on their websites: WorldClim, Geospatial Interactive Online Visualization and Analysis Infrastructure, and South African Weather Service (climate data), United States Geological Survey (Landsat images), City of Cape Town (vegetation data), and South African National Parks (wildfire occurrence data). We appreciate the anonymous reviewers, for their constructive comments, suggestions and questions that have been used to improve the quality of this manuscript.

6. References

Abdo, H. G., Almohamad, H., Al Dughairi, A. A., & Al-Mutiry, M. (2022). GIS-Based Frequency Ratio and Analytic Hierarchy Process for Forest Fire Susceptibility Mapping in the Western Region of Syria. *Sustainability*, *14*(8), 4668. [Crossref]

Carlson, T. N., & Ripley, D. A. (1997). On the Relation etween NDVI, Fractional Vegetation Cover, and Leaf Area Index. *Remote Sensing of Environment*, *62*(3), 241–252. [Crossref]

Chapungu, L., Nhamo, G., Chikodzi, D., & Dube, K. (2024). Trends and Impacts of Temperature and Fire Regimes in South Africa's Coastal National Parks: Implications for Tourism. *Natural Hazards*, *120*(5), 4485–4506. [Crossref]

Cowling, R. M., MacDonald, I. A. W., & Simmons, M. T. (1996). The Cape Peninsula, South Africa: Physiographical, Biological and Historical Background to an Extraordinary Hot-Spot of Biodiversity. *Biodiversity & Conservation*, *5*(5), 527–550. [Crossref]

Cruz, M. G., & Alexander, M. E. (2019). The 10% Wind Speed Rule of Thumb for Estimating a Wildfire's Forward Rate of Spread in Forests and Shrublands. *Annals of Forest Science*, *76*(2), 44. [Crossref]

Defratti, M., Scholar, M., & Yarnal, B. (2015). Analyzing Fire Hazard Risk: A Case Study in Table Mountain National Park, Cape Town, South Africa. *The Penn State McNair Journal*, *20*, 36–46.

Forsyth, G. G., & van Wilgen, B. W. (2008). The Recent Fire History of the Table Mountain National Park and Implications for Fire Management. *Koedoe*, *50*(1). [Crossref]

Holden, Z. A., Swanson, A., Luce, C. H., Jolly, W. M., Maneta, M., Oyler, J. W., Warren, D. A., Parsons, R., & Affleck, D. (2018). Decreasing Fire Season Precipitation Increased Recent Western US Forest Wildfire Activity. *Proceedings of the National Academy of Sciences*, *115*(36). [Crossref]

Imray, G. (2021). *Cape Town Wildfire Largely Contained, Damage is Assessed*. AP NEWS. https://apnews.com/article/cape-town-fire-largely-contained-54346dfc0c26ae6ba51eb893ac1f59c0

Kavlak, M. O., Cabuk, S. N., & Cetin, M. (2021). Development of Forest Fire Risk Map Using Geographical Information Systems and Remote Sensing Capabilities: Ören Case. *Environmental Science and Pollution Research*, *28*(25), 33265–33291. [Crossref]

Kayet, N., Chakrabarty, A., Pathak, K., Sahoo, S., Dutta, T., & Hatai, B. K. (2020). Comparative Analysis of Multi-Criteria Probabilistic FR and AHP Models for Forest Fire Risk (FFR) Mapping in Melghat Tiger Reserve (MTR) Forest. *Journal of Forestry Research*, *31*(2), 565–579. [Crossref]

Kruger, L. M., Midgley, J. J., & Cowling, R. M. (1997). Resprouters vs Reseeders in South African Forest Trees; A Model based on Forest Canopy Height. *Functional Ecology*, *11*(1), 101–105. [Crossref]

Kumari, B., & Pandey, A. C. (2020). Geo-Informatics based Multi-Criteria Decision Analysis (MCDA) Through Analytic Hierarchy Process (AHP) for Forest Fire Risk Mapping in Palamau Tiger Reserve, Jharkhand State, India. *Journal of Earth System Science*, *129*(1), 204. [Crossref]

Lasslop, G., Hantson, S., Harrison, S. P., Bachelet, D., Burton, C., Forkel, M., Forrest, M., Li, F., Melton, J. R., Yue, C., Archibald, S., Scheiter, S., Arneth, A., Hickler, T., & Sitch, S. (2020). Global Ecosystems and F: Multi-Model Assessment of Fire-Induced Tree-Cover and Carbon Storage Reduction. *Global Change Biology*, *26*(9), 5027–5041. [Crossref]

Malindi, M., & Odera, P. A. (2021). An Assessment of SRTM, ASTER and LiDAR Digital Elevation Models in the Western Part of South Africa. *Journal of Geomatics*, *15*(2), 115–120.

Marais, K. E., Pratt, R. B., Jacobs, S. M., Jacobsen, A. L., & Esler, K. J. (2014). Postfire Regeneration of Resprouting Mountain Fynbos Shrubs: Differentiating Obligate Resprouters and facultative seeders. *Plant Ecology*, *215*(2), 195–208. [Crossref]

Mayfield, C. J., Kumler, M., & Afzalan, N. (2015). Automating the Classification of Thematic Rasters for Weighted Overlay Analysis in GeoPlanner for ArcGIS. *InSPIRe @ Redlands MS*.

McLauchlan, K. K., Higuera, P. E., Miesel, J., Rogers, B. M., Schweitzer, J., Shuman, J. K., Tepley, A. J., Varner, J. M., Veblen, T. T., Adalsteinsson, S. A., Balch, J. K., Baker, P., Batllori, E., Bigio, E., Brando, P., Cattau, M., Chipman, M. L., Coen, J., Crandall, R., … Watts, A. C. (2020). Fire as a Fundamental Ecological Process: Research Advances and Frontiers. *Journal of Ecology*, *108*(5), 2047–2069. [Crossref]

Nones, M., Hamidifar, H., & Shahabi-Haghighi, S. M. B. (2024). Exploring EM-DAT for Depicting Spatiotemporal Trends of Drought and Wildfires and their Connections with Anthropogenic Pressure. *Natural Hazards*, *120*(1), 957–973. [Crossref]

Novo, A., Fariñas-Álvarez, N., Martínez-Sánchez, J., González-Jorge, H., Fernández-Alonso, J. M., & Lorenzo, H. (2020). Mapping Forest Fire Risk—A Case Study in Galicia (Spain). *Remote Sensing*, *12*(22), 3705. [Crossref]

Nuthammachot, N., & Stratoulias, D. (2021). A GIS and AHP-Based Approach to Map Fire Risk: A Case Study of Kuan Kreng Peat Swamp Forest, Thailand. *Geocarto International*, *36*(2), 212–225. [Crossref]

Pausas, J. G., & Keeley, J. E. (2021). Wildfires and Global Change. *Frontiers in Ecology and the Environment*, *19*(7), 387–395. [Crossref]

Pourtaghi, Z. S., Pourghasemi, H. R., & Rossi, M. (2015). Forest Fire Susceptibility Mapping in the Minudasht Forests, Golestan Province, Iran. *Environmental Earth Sciences*, *73*(4), 1515–1533. [Crossref]

Saaty, T. L. (2004). Decision Making — the Analytic Hierarchy and Network Processes (AHP/ANP). *Journal of Systems Science and Systems Engineering*, *13*(1), 1–35. [Crossref]

Shoko, M., & Gayu, E. K. (2021). *Digital Models for Planning and Disaster Management*. GIM International. https://www.gim-international.com/content/article/digital-models-for-planning-and-disaster-management

Sivrikaya, F., & Küçük, Ö. (2022). Modeling Forest Fire Risk Based on GIS-Based Analytical Hierarchy Process and Statistical Analysis in Mediterranean Region. *Ecological Informatics*, *68*, 101537. [Crossref]

Suryabhagavan, K. V, Alemu, M., & Balakrishnan, M. (2016). GIS-Based Multi-Criteria Decision Analysis for Forest Fire Susceptibility Mapping: A Case Study in Harenna Forest Southwestern Ethiopia. *Tropical Ecology*, *57*(1), 33–43.

Tiwari, A., Shoab, M., & Dixit, A. (2021). GIS-Based Forest Fire Susceptibility Modeling in Pauri Garhwal, India: A Comparative Assessment of Frequency Ratio, Analytic Hierarchy Process and fuzzy modeling techniques. *Natural Hazards*, *105*(2), 1189–1230. [Crossref]

Urbanski, S. P., Hao, W. M., & Baker, S. (2008). *Chapter 4 Chemical Composition of Wildland Fire Emissions* (pp. 79–107). [Crossref]

van Wilgen, B. W. (2015). Dealing with the inevitable: Fire on Table Mountain. *South African Journal of Science*, *111*(1/2), 1–2. [Crossref]

Velizarova, E., Nedkov, R., Molla, I., & Zaharinova, M. (2017). Application of Aerospace Data for Forest Fire Risk Assessment and Prognoses. A Case Study for Vitosha Mountain. *Ecological Engineering and Environment Protection*, *1*, 38–45. [Crossref]

Ya'acob, N., Jamil, I. A. A., Aziz, N. F. A., Yusof, A. L., Kassim, M., & Naim, N. F. (2022). Hotspots Forest Fire Susceptibility Mapping for Land Use or Land Cover using Remote Sensing and Geographical Information Systems (GIS). *IOP Conference Series: Earth and Environmental Science*, *1064*(1), 012029. [Crossref]